NASA/TM—2011-216367 AIAA–2009–4263

Icing Encounter Duration Sensitivity Study

Harold E. Addy, Jr.
Glenn Research Center, Cleveland, Ohio

Sam Lee
ASRC Aerospace Corporation, Cleveland, Ohio

March 2011

NASA STI Program . . . in Profile

Since its founding, NASA has been dedicated to the advancement of aeronautics and space science. The NASA Scientific and Technical Information (STI) program plays a key part in helping NASA maintain this important role.

The NASA STI Program operates under the auspices of the Agency Chief Information Officer. It collects, organizes, provides for archiving, and disseminates NASA's STI. The NASA STI program provides access to the NASA Aeronautics and Space Database and its public interface, the NASA Technical Reports Server, thus providing one of the largest collections of aeronautical and space science STI in the world. Results are published in both non-NASA channels and by NASA in the NASA STI Report Series, which includes the following report types:

- TECHNICAL PUBLICATION. Reports of completed research or a major significant phase of research that present the results of NASA programs and include extensive data or theoretical analysis. Includes compilations of significant scientific and technical data and information deemed to be of continuing reference value. NASA counterpart of peer-reviewed formal professional papers but has less stringent limitations on manuscript length and extent of graphic presentations.

- TECHNICAL MEMORANDUM. Scientific and technical findings that are preliminary or of specialized interest, e.g., quick release reports, working papers, and bibliographies that contain minimal annotation. Does not contain extensive analysis.

- CONTRACTOR REPORT. Scientific and technical findings by NASA-sponsored contractors and grantees.

- CONFERENCE PUBLICATION. Collected papers from scientific and technical conferences, symposia, seminars, or other meetings sponsored or cosponsored by NASA.

- SPECIAL PUBLICATION. Scientific, technical, or historical information from NASA programs, projects, and missions, often concerned with subjects having substantial public interest.

- TECHNICAL TRANSLATION. English-language translations of foreign scientific and technical material pertinent to NASA's mission.

Specialized services also include creating custom thesauri, building customized databases, organizing and publishing research results.

For more information about the NASA STI program, see the following:

- Access the NASA STI program home page at *http://www.sti.nasa.gov*

- E-mail your question via the Internet to *help@sti.nasa.gov*

- Fax your question to the NASA STI Help Desk at 443–757–5803

- Telephone the NASA STI Help Desk at 443–757–5802

- Write to:
  NASA Center for AeroSpace Information (CASI)
  7115 Standard Drive
  Hanover, MD 21076–1320

NASA/TM—2011-216367 AIAA–2009–4263

Icing Encounter Duration Sensitivity Study

Harold E. Addy, Jr.
Glenn Research Center, Cleveland, Ohio

Sam Lee
ASRC Aerospace Corporation, Cleveland, Ohio

Prepared for the
First Atmospheric and Space Environments Conference
sponsored by the American Institute of Aeronautics and Astronautics
San Antonio, Texas, June 22–25, 2009

National Aeronautics and
Space Administration

Glenn Research Center
Cleveland, Ohio 44135

March 2011

Acknowledgments

The authors would like to thank the crew of the IRT for providing expert assistance throughout the tests, Julius Mirecki for setting up the measurement systems and providing support for the data acquisition, and to Andy Broeren for providing key insight and suggestions during data analysis.

Level of Review: This material has been technically reviewed by technical management.

Available from

NASA Center for Aerospace Information
7115 Standard Drive
Hanover, MD 21076–1320

National Technical Information Service
5301 Shawnee Road
Alexandria, VA 22312

Available electronically at http://www.sti.nasa.gov

Icing Encounter Duration Sensitivity Study

Harold E. Addy, Jr.
National Aeronautics and Space Administration
Glenn Research Center
Cleveland, Ohio 44135

Sam Lee
ASRC Aerospace Corporation
Cleveland, Ohio 44135

Abstract

This paper describes a study performed to investigate how aerodynamic performance degradation progresses with time throughout an exposure to icing conditions. It is one of the first documented studies of the effects of ice contamination on aerodynamic performance at various points in time throughout an icing encounter. Both a 1.5 and a 6 ft chord, two-dimensional, NACA-23012 airfoils were subjected to icing conditions in the NASA Icing Research Tunnel (IRT) for varying lengths of time. At the end of each run, lift, drag, and pitching moment measurements were made. Measurements with the 1.5 ft chord model showed that maximum lift and pitching moment degraded more rapidly early in the exposure and degraded more slowly as time progressed. Drag for the 1.5 ft chord model degraded more linearly with time, although drag for very short exposure durations was slightly higher than expected. Only drag measurements were made with the 6 ft chord airfoil. Here, drag for the long exposures was higher than expected. Novel comparison of drag measurements versus an icing scaling parameter, accumulation parameter times collection efficiency was used to compare the data from the two different size models. The comparisons provided a means of assessing the level of fidelity needed for accurate icing simulation.

Nomenclature

Ac	accumulation parameter
AoA	angle of attack, deg
beta	collection efficiency
c	chord
cd	drag coefficient
*cd*0	drag coefficient, clean airfoil
Cl	lift coefficient
Clm	maximum lift coefficient
*Clm*0	maximum lift coefficient, clean airfoil
Cm	pitching moment coefficient
F	Fahrenheit *k* = ice height
LWC	liquid water content, grams/cubic meter
MVD	median volumetric diameter, micrometers
Re	Reynolds number
V	airspeed, knots

Introduction

Airfoil and aircraft performance degradation due to inflight icing is a widely known aviation hazard. Over the last two decades, studies (Refs. 1 to 17) have been conducted to investigate and measure the effect ice accretions have on the aerodynamic performance of airfoils and wings. Various aspects of the problem have been considered including the type of ice, the fidelity of the ice shapes, and the type of airfoil. Little has been done, however, to study how aerodynamic performance degrades with time as the ice initially begins to accrete on an airfoil and then grows as the icing encounter continues.

One study that did investigate aerodynamic performance degradation with time as ice continued to accrete was conducted by Potapczuk and Berkowitz in 1990 (Ref. 17). Using a two-dimensional multi-element airfoil model mounted on a force balance in the NASA Glenn Research Center's Icing Research Tunnel (IRT), measurements of lift, drag, and pitching moment were made as ice accreted on the model. Large degradations in performance were measured. The degradations, however, were typically not linear with time. In general, the initial ice accretions contributed more to the overall degradation than ice accreted later during the icing encounter.

The Potapczuk and Berkowitz study, however, did not attempt to measure icing effect on maximum lift coefficient or stall angle throughout the accretion. These measurements were made only at the end of the allotted ice accretion time. Another aspect of the Potapczuk and Berkowitz study was that it was performed on a subscale model. Because ice accretes differently on a subscale model than on a full scale model, there can be different aerodynamic effects. The considerable resources required for a full scale investigation were unavailable for that study, although the results were still very valuable.

The investigation described in this paper was designed to address the outstanding questions left by the Potapczuk and Berkowitz study. Airfoil aerodynamic performance measurements were made after various lengths of exposure to icing conditions. Both subscale and full scale, two-dimensional models were tested. The icing conditions remained the same throughout the test for each model, only the length of exposure was varied. For the iced subscale model, lift and pitching moment measurements were made at multiple angles of attack from zero through maximum lift. Drag measurements were made at selected angles of attack for both models with ice accreted.

Test Description

This study included two test campaigns in the NASA Glenn Icing Research Tunnel. The first was conducted using a two-dimensional, subscale, 1.5 ft chord, NACA-23012 model. The second campaign used a full-scale, 6 ft chord version of the same airfoil. The models had been used in prior ice accretion and iced-aerodynamic performance studies, so existing databases could be leveraged to verify and corroborate data collected in this study. The models were exposed to selected icing conditions in the IRT for several different periods of time. At the conclusion of each exposure period, aerodynamic performance measurements were made and then the ice accretions were documented using ice tracings, photographs, and ice depth measurements.

First Campaign

The first test used the 1.5 ft chord NACA-23012 model. There were two reasons for testing this model in the first campaign. First, its size, in comparison with the dimensions of the test section of the IRT, allowed lift and pitching moment data to be taken free of large wall and blockage interference effects. Secondly, since high-quality aerodynamic performance measurements had been made in a low-speed aerodynamic tunnel using castings of ice shapes accreted at some of the same conditions as those in this study, the quality of the performance measurements in the IRT could be verified.

A photograph of the 1.5 ft chord model mounted vertically in the IRT is shown in Figure 1. It was made from solid aluminum and had a row of pressure taps located about 18 in. above the floor of the tunnel. These pressure taps were used to align the clean model to the airflow and obtain clean model lift

Figure 1.—1.5 ft chord model in IRT.

and pitching moment coefficients. Because the taps around the leading edge of the models iced over during exposure to the icing cloud, the pressure measurements were not used to make lift and pitching moment calculations after ice was accreted.

The model was mounted on an external force balance located just below the floor and above the ceiling of the tunnel. The measurements of lift and pitching moment with ice accreted on the model were made using this force balance system. Conventional two-dimensional wind tunnel model corrections (Ref. 18) were applied to all the performance data. Drag measurements were made using a traversing wake survey system mounted on the floor downstream of the model.

Icing Research Tunnel

The IRT is an atmospheric wind tunnel with a test section 6 ft high by 9 ft wide and 20 ft long. It is capable of airspeeds up to 400 mph (test section empty), Mach numbers to about 0.45, and Reynolds numbers of three million per foot. Air temperatures can be cooled to –20 °F.

It can produce an icing cloud with droplet sizes and liquid water contents similar to those prescribed in the FAA's CFR Appendix C aircraft certification icing cloud specifications. It can also produce supercooled large droplets (SLD) over a range of droplet sizes and liquid water contents.

The ability of the IRT to repeat ice shapes for a given set of icing conditions is well established (Ref. 22). Tracings were made of select repeat conditions to ensure measurements were being made with like ice accretions.

A difficulty with making aerodynamic performance measurements in an icing wind tunnel is that these tunnels typically have high freestream turbulence levels in comparison with dry, aerodynamic wind tunnels. The cloud generating equipment present in the tunnel is one of the reasons for this. Moreover, it is not unusual for equipment to be added to an icing tunnel specifically to increase air turbulence to make the icing cloud more uniform. A uniform icing cloud is often more important to icing tests than elevated turbulence. Finally, to prevent the water droplet generating equipment (i.e., water spray systems) from freezing, air is continuously blown through the droplet-generating nozzles, thereby generating additional air turbulence. Turbulence in the IRT has been measured at about 1.0 percent with spray bar air activated (Ref. 19).

Test Setup

The 1.5 ft chord model was mounted vertically on the turntable and force balance in the test section of the IRT and spanned the 6 ft from floor to ceiling. A traversing drag wake survey system was mounted to the floor of the tunnel about two chord lengths downstream of the model's trailing edge.

The icing condition selected was a glaze ice condition from the CFR Appendix C envelope. Glaze ice accreted on the leading edge of an airfoil typically produces a high degree of performance degradation, so a study of how this degradation changes with time of exposure is of particular interest. For the 1.5 ft chord model, a cloud with droplets of 15 μm in median volumetric diameter (MVD) and with a liquid water content (LWC) of 0.75 gm^3 was chosen. The models were set at an angle-of-attack (AOA) of 2°. The airspeed was 200 knots and the air total air temperature was 28 °F. This condition had been used in a previous study where aerodynamic performance measurements were made in a dry wind tunnel using castings. This allowed iced performance measurements made in the IRT to be compared with similar measurements in another tunnel. The cloud covered most, but not all, of the model span. The ice accretions started at about 6 in. from the ceiling and ended about 3 in. from the floor of the tunnel.

Another difficulty discovered during the tests was that at the 200 knot airspeed at which the ice was accreted, the wake survey probe tip tended to ice up due to a very faint cloud of very small (<10 μm diameter) water droplets circulating with the air in the tunnel. These droplets are so small and constitute such a low LWC that they do not affect most tests in the IRT. However, they do form small accretions on smaller objects with sharp edges where the collection efficiency is very high. The tip of the wake survey probe is heated to prevent ice buildup, but, at 200 knots and 28 °F, the convective cooling of the tip is sufficient to permit ice accretion. Lowering the airspeed to 150 knots allowed the wake survey tip to remain warm enough to prevent any ice accretion. Therefore, ice was first accreted on the model at the stated conditions, and then the tunnel airspeed was lowered to 150 knots where the aerodynamic performance data were acquired. This was done for both the first and second campaigns of this study. The Mach number at this speed and temperature was 0.235. The Reynolds numbers were 2.6 and 10.4 million for the 1.5 and 6 ft chord models, respectively.

A final challenge for these tests was that once the cloud in the IRT was shut off, the accreted ice would slowly begin to sublimate or erode, or both. This meant that if it took a long time to acquire the performance data, the ice accretion at the end of the data acquisition was different than at the beginning. Since taking a complete set of performance data could be time consuming, ice accretions were often repeated acquiring partial data sets each time, in order to acquire a complete set of data.

Force balance data were often collected at four to six angles-of-attack at a time for each ice accretion. Data were taken mostly around stall. Wake survey data were taken at four angles-of-attack, 0°, 2°, 4°, and 6°. It usually required two ice accretions to acquire the wake survey data for a particular icing exposure time.

Measurement Errors

An error analysis of the algorithm and the pressure instrumentation used to calculate the drag coefficients show that the uncertainty for these values is ±12 drag counts where one drag count is an increment of 0.0001 in drag coefficient. While relatively high for clean airfoil drag measurements, it is a reasonable level for ice-contaminated airfoils where the drag coefficients are typically much higher.

A static calibration of the force balance has shown the accuracy of this measurement system to be ±3 percent in lift and ±10 percent in pitching moment. It has been noted (Ref. 20), however, that for two-dimensional wind tunnel tests where a constant chord model completely spans the test section, the spanwise distribution of lift caused by the tunnel walls diminishes lift by, typically, 10 to 15 percent at maximum lift coefficient. This has been observed in the IRT (Ref. 7).

A further potential complication exists when using the force balance in the icing tunnel. As was mentioned previously, the icing cloud does not cover the entire span of the model, but the force balance measures the forces over the entire model. Therefore, some error is introduced into the assumption of infinite span, as is the case in full span, two-dimensional model testing.

An error analysis (Ref. 7) of the data measurements indicates that the lift coefficients calculated from the surface pressures have an uncertainty of approximately ±2 percent up to the maximum lift coefficient and ±4 percent for pitching moment.

First Campaign Results

Because aerodynamic performance measurements are not often made in an icing wing tunnel, in addition to establishing system component error, the repeatability of the measurements was documented. Figure 2 shows lift and pitching moment coefficients for the clean model as measured by the force balance on four different days of testing. As can be seen, the repeatability was very good. Similar repeatability curves for the pressure tap measurements are shown in Figure 3. Data from Run 210 were not shown because water had contaminated the pressure lines from the taps to the transducers. The water was subsequently cleared.

Repeat runs were not made with the wake survey for the clean model due primarily to the large investment of test time required to run a survey. However, repeat wake surveys were run for the iced airfoil. These data are shown in Figure 4. Again, the repeatability is good.

Also to increase confidence in the data, measurements were compared with data measured at the University of Illinois at Urbana-Champaign's Low Speed Wind Tunnel (LSWT). Figure 5 shows a comparison of lift and pitching moment coefficients as measured by both the force balance and the surface pressures in the IRT with those measured in the LSWT using the surface pressure method.

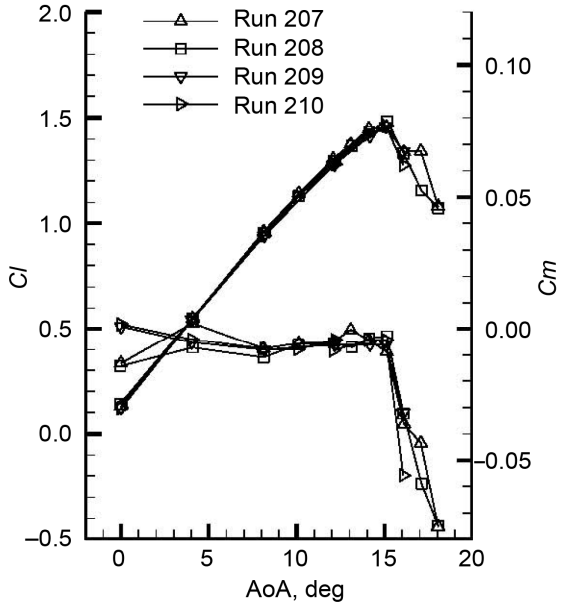

Figure 2.—Repeat force balance measurements in the IRT.

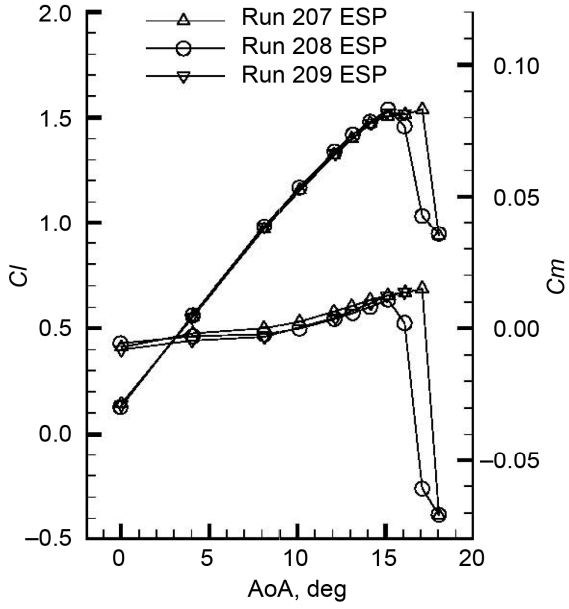

Figure 3.—Repeat surface pressure measurements in the IRT.

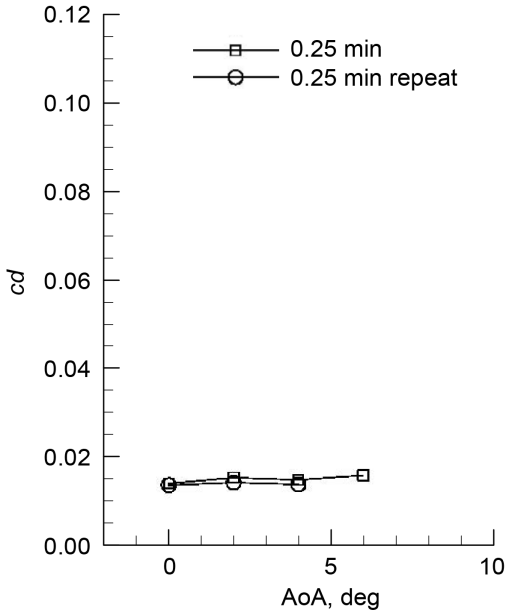

Figure 4.—Repeat wake survey measurements in the IRT.

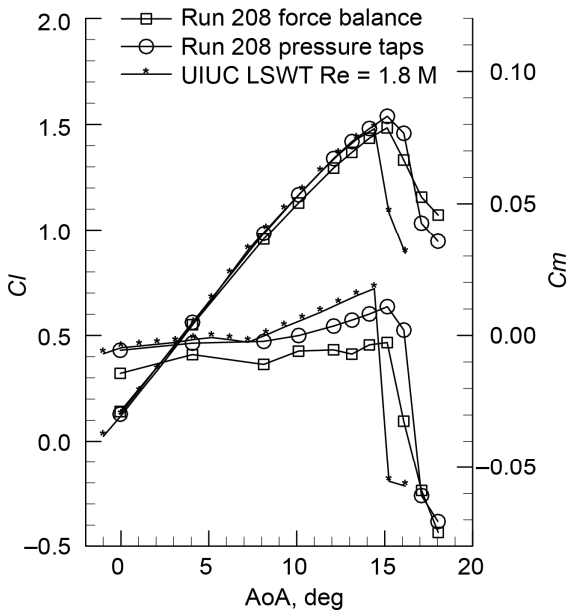

Figure 5.—Clean model measurements in the IRT and LSWT.

The models in both tests were 1.5 ft chord, NACA-23012 models. However, the model used in the LSWT had a span of 34 in., rather than the 6 ft span of the IRT model. Also, the data were collected at differing Reynolds numbers. The LSWT data were collected at a Re = 1.8 million while the IRT data were collected at Re = 2.35 million. The difference in Reynolds number explains the lower maximum lift coefficient and earlier stall angle for the LSWT test. This is illustrated in Figure 6 where data from tests conducted by the UIUC of a NACA-23012 airfoil in NASA Langley's Low Turbulence Pressure Tunnel (LTPT) is compared with data from the current study in the IRT. The pressure capability of the LTPT allowed independent variation of Mach and Reynolds numbers. The IRT data were acquired at a Reynolds number of 2.6 million, while the data shown from the LTPT are from Reynolds numbers of 2.0 and 3.5 million. As expected, the IRT data falls in between the data from the LTPT.

The difference in the lift coefficients near maximum lift between the force balance and surface pressure measurements in the IRT is likely due to airflow at the floor and ceiling of the IRT which causes a decrease in the lifting force on the airfoil. This decrease is measured by the force balance but not by the surface pressure taps which measure only section lift at a station 18 in. above the floor. The difference in pitching moment coefficients between the force balance and surface pressure measurements in the IRT is likely due to the inaccuracy of the force balance measurement. To obtain the pitching moment, the force balance must discern a small difference in two much larger forces and then multiply the difference by the moment arm. The error band becomes relatively large in these circumstances. Nonetheless, the trends are correct.

A comparison of clean model drag wake survey results for the IRT and LSWT tests is shown in Figure 7. Drag coefficients measured in the IRT are slightly higher likely due to the higher turbulence levels in the IRT. The higher Reynolds number at which the IRT data were taken may also contribute to the higher IRT results.

Iced Airfoil Results

For the 1.5 ft chord model, aerodynamic performance measurements were made after icing exposure times of 0.25, 0.5, 1.0, 2.5, and 5.0 min. The ice accreted during the latter four of these exposure times is shown in the ice tracings of Figures 8(a) to (d). No tracing or ice depth measurement was made of the 0.25 min exposure ice accretion because the amount of ice was too small.

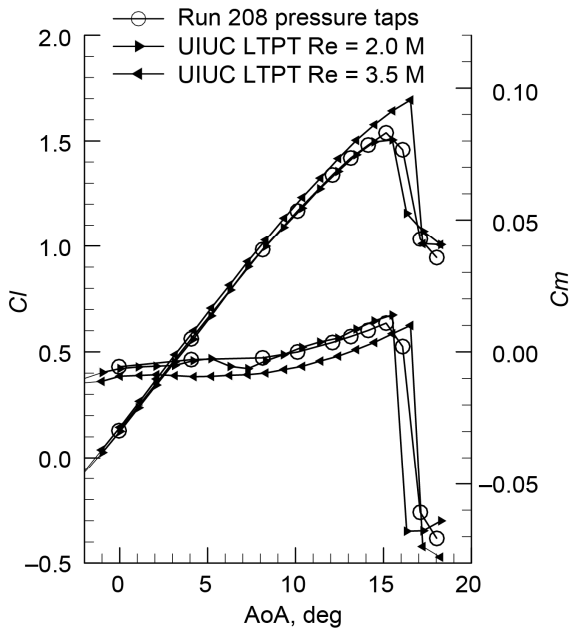

Figure 6.—Clean model measurements in the IRT and LTPT.

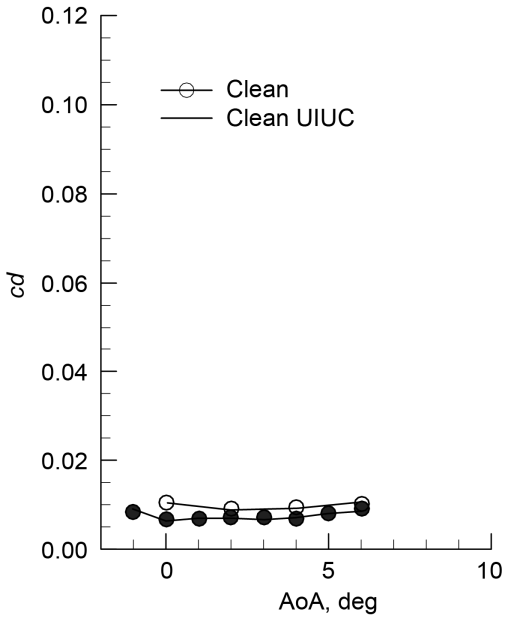

Figure 7.—Clean model drag measurements in the IRT and LSWT.

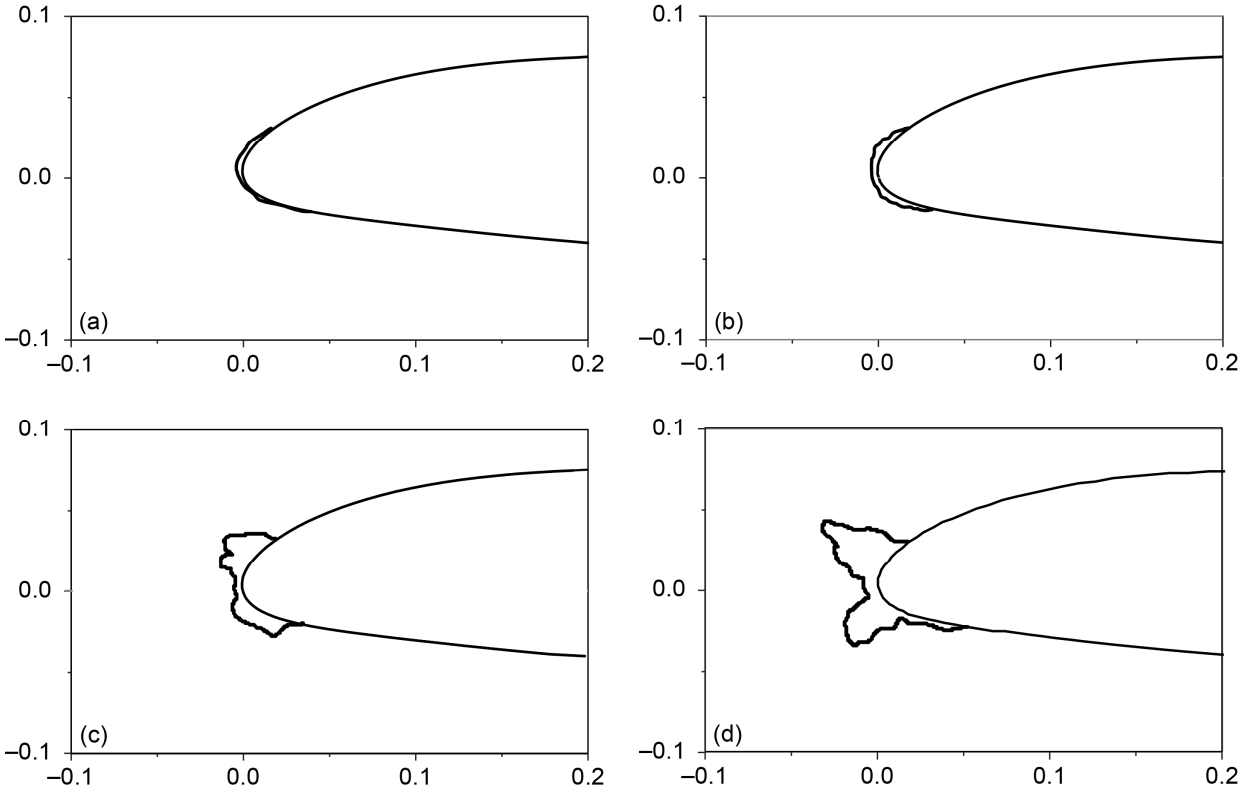

Figure 8.—Ice accretion on 1.5 ft chord model. (a) 0.5 min. (b) 1.0 min. (c) 2.5 min. (d) 5.0 min.

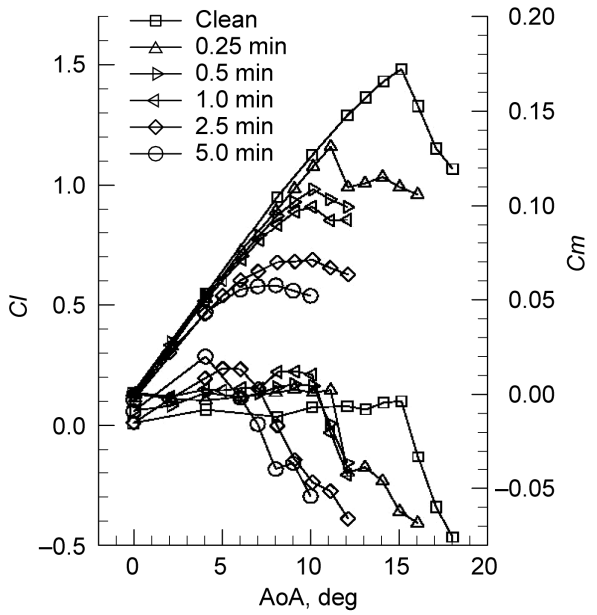

Figure 9.—Effect of ice on lift and pitching moment coefficients for 1.5 ft chord model.

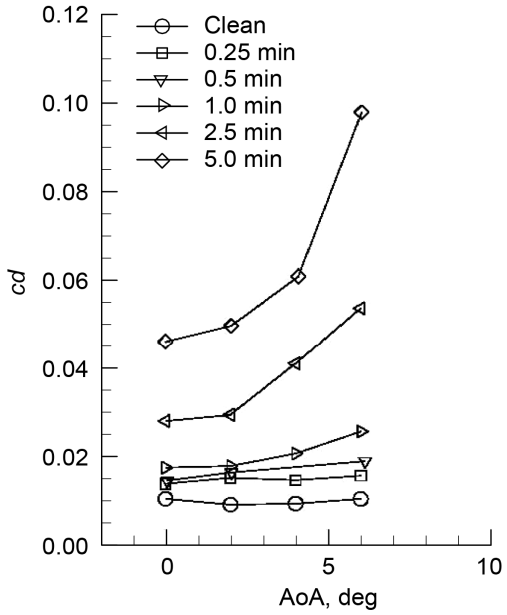

Figure 10.—Effect of ice on drag coefficient for 1.5 ft chord model.

Force balance measurements made for these ice accretions are shown in Figure 9. Even the very small amount of ice accreted during the 0.25 min exposure had a dramatic effect on maximum lift coefficient and stall angle. Note, however, that the leading edge stall exhibited by the airfoil for this small amount of ice is the same as for the clean airfoil. At 0.5 min of ice accretion, maximum lift coefficient and stall angle are further diminished, but a different type of stall is indicated by the less-abrupt decrease in the lift curve. At the Reynolds number of 2.6 million at which these data was obtained, it is likely that a thin airfoil-type stall occurred. The effects of glaze ice on lift and pitching moment for this airfoil are dramatic. The 5 min. ice accretion reduced maximum lift to 38 percent of the clean airfoil's value.

The pitching moment curves for each of these ice accretions are also shown in Figure 9. These data also reflect the dramatic effect such ice accretions have on the aerodynamic performance of this model. Note here also, that the very short icing exposure time of only 0.25 min causes the pitching moment to go strongly negative at a much lower angle of attack than for the clean airfoil.

The drag data for these ice accretions also show dramatic aerodynamic performance degradation as shown in Figure 10. Again, a relatively large increase in drag was caused by the small, 0.25 min ice accretion.

As was mentioned earlier, some of the ice accretions matched ice accretions from a previous test where ice castings were made and subsequently tested in the dry, aerodynamic, LSWT at UIUC. The performance data from those tests are compared with the IRT data in Figures 11 and 12. The lift coefficients for the 0.5 min ice accretion and casting agree very well even though the Reynolds numbers for the two cases are different. In several two-dimensional airfoil tests with leading edge ice, however, it has been shown that Reynolds number effects are negated by the presence of the ice on the leading edge of the model (Refs. 5, 6, and 12). There is some difference in the lift coefficients for the 5 min ice shape around maximum lift with the IRT values showing greater degradation. However, the lift curves are very similar in shape indicating a similar stall behavior.

The drag coefficients agree fairly well for the 0.5 min ice accretion at IRT and the corresponding casting at LSWT. Similar to the lift coefficients results for the 5.0 min ice shapes, the IRT accretion shows greater performance degradation in comparison with the LSWT results.

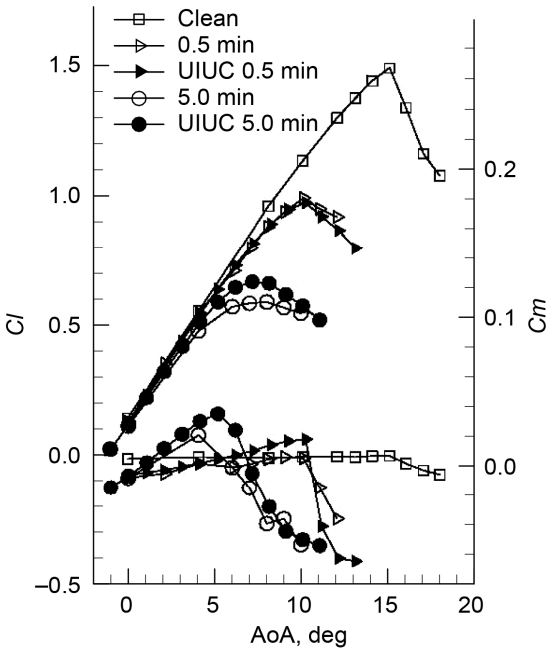

Figure 11.—Comparison of IRT ice accretion and LSWT ice casting data.

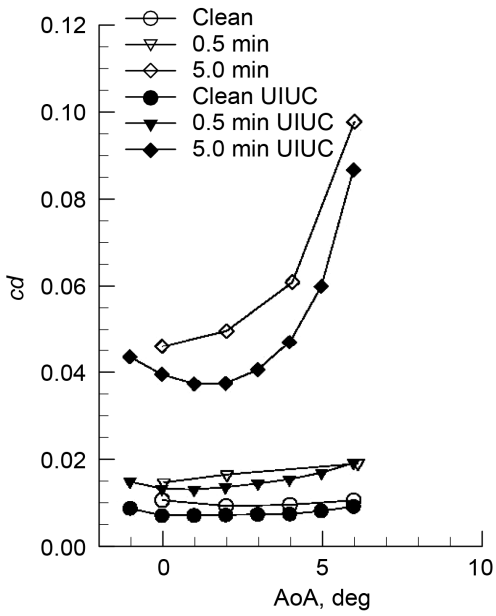

Figure 12.—Comparison of IRT ice accretion and LSWT ice casting drag data.

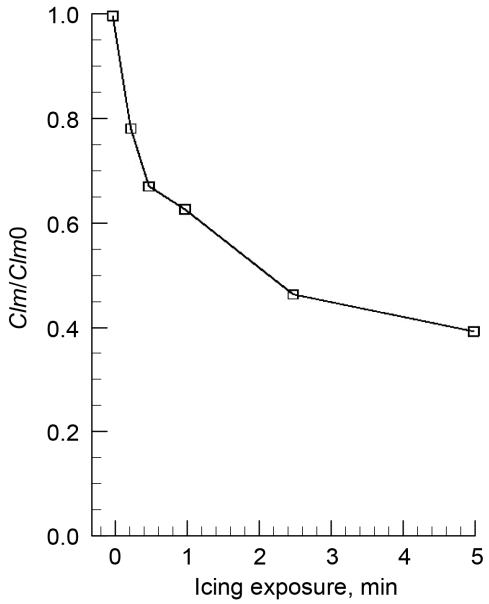

Figure 13.—Maximum lift degradation as a function of exposure time.

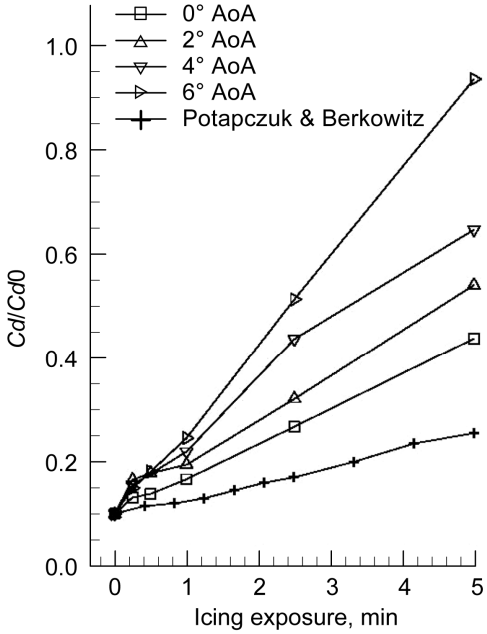

Figure 14.—Drag degradation as a function of exposure time.

Another way to look at performance degradation with exposure time is to plot maximum lift coefficient and drag coefficient, each normalized by its appropriate uncontaminated model value, as a function of exposure time. Figure 13 shows this plot for maximum lift coefficient normalized by the maximum lift coefficient for the clean model. The curve is roughly asymptotic, indicating diminishing maximum lift coefficient degradation with exposure time.

Figure 14 shows drag coefficients normalized by the appropriate clean model drag coefficient as a function of exposure time for each of the four angles of attack at which wake survey measurements were taken. For each angle of attack, the drag coefficients form approximately straight lines. In contrast to lift

degradation, the drag degrades linearly with exposure time. There is, however, a modest, but noticeable bump up in the drag versus exposure time curves for the very short exposure time of 0.25 min. This short exposure time is not long enough to allow the airfoil's surface to become thoroughly wetted. The appearance of the ice accreted is patchy and somewhat rough and does not completely cover the leading edge of the airfoil. The patchy roughness of the ice is likely more a function of the water surface tension and airfoil surface character and is less dependent on the size of the model. This raises the question of whether the initial ice roughness on the leading edge of the model is disproportionately large for a small subscale model.

Also shown in Figure 14 are drag data from one of the Potapczuk and Berkowitz tests. Although the model, icing conditions, and ice accretion are different, the trend is similar.

Second Campaign Results

A second test campaign was conducted in the IRT using a 6 ft chord, two-dimensional NACA-23012 airfoil in order to obtain reference data for the small scale, 1.5 ft chord model tests. The performance degradation due to the short icing exposures of the 1.5 ft chord model seemed inordinately high. Running tests with a 6 ft chord model could help determine whether the initial ice accretion was creating an ice roughness that was disproportionately large for the size of the 1.5 ft chord model.

Like the 1.5 ft chord model, the 6 ft chord model was also machined from solid aluminum and had a chord-wise row of pressure taps located 18 in. above the tunnel floor on the vertically mounted model. A photo of the model installed in the test section of the IRT is shown in Figure 15.

Figure 15.—6 ft chord NACA-23012 model in IRT.

Aerodynamic performance measurements were limited with the 6 ft chord model for several reasons. First, the model could not be mounted on the IRT's external force balance due to the manner in which its attachment points were constructed. Secondly, due to the large blockage created by the model in the tunnel, it could not be rotated through stall. Finally, as was the case for the 1.5 ft chord model, when ice was accreted, the leading edge surface pressure taps were covered, preventing lift and pitching moment calculations. Therefore, only drag measurements were made at select low angles of attack for the clean and iced model and lift and pitching moment for the clean model. Drag was measured using the same wake survey system as used in the first campaign.

The icing conditions selected for the second campaign were different from those used in the first campaign due primarily to the difference in collection efficiencies of the two models. The icing conditions for the two campaigns are shown in Table 1 along with the collection efficiencies for the two models and the accumulation parameters for the different cases.

TABLE 1.—ICING CONDITIONS FOR THE IRT CAMPAIGNS

Two-dimensional NACA-23012									
Chord	MVD	LWC	V	AoA	Exposure time	Accumulation parameter	Collection efficiency	Ac-beta	Similar cases
ft	m^{-6}	g/m^3	kt	deg	min	Ac	beta		
1.5	15.4	0.75	200	2	0.25	0.087	0.701	0.061	A
1.5	15.4	0.75	200	2	0.5	0.17	0.701	0.12	B
1.5	15.4	0.75	200	2	1	0.35	0.701	0.25	C
1.5	15.4	0.75	200	2	2.5	0.87	0.701	0.61	D
1.5	15.4	0.75	200	2	5	1.7	0.701	1.2	
6	20	0.5	200	2	1	0.058	0.511	0.030	
6	20	0.5	200	2	2	0.12	0.511	0.060	A
6	20	0.5	200	2	5	0.29	0.511	0.15	B
6	20	0.5	200	2	7.5	0.44	0.511	0.22	C
6	20	0.5	200	2	10	0.58	0.511	0.30	
6	20	0.5	200	2	15	0.87	0.511	0.45	
6	20	0.5	200	2	22.5	1.3	0.511	0.67	D

Collection efficiencies and accumulation parameters (Ref. 21), along with their product, Ac-beta, were calculated for the different cases to obtain geometrically similar ice shapes for the two different size models. The cases A, B, C, and D in the table are pairs of geometrically similar ice accretions. Tracings of the ice shapes for the 6 ft chord model test are shown in Figures 16(a) to (d). The ice accretions for the 1 and 2 min cases for the 6 ft chord model were too small to trace.

To raise confidence in the aerodynamic measurements in the IRT, the IRT data were compared with data taken in a dry aerodynamic tunnel in another program. In an iced aerodynamic simulation program conducted jointly with NASA, ONERA, and UIUC participation, a two-dimensional, 6 ft chord, NACA-23012 airfoil was tested both clean and with cast ice shapes in ONERA's F1 tunnel at Fauga-Mauzac. Drag data from clean models are compared in Figure 17, while drag data from the ice-contaminated models are compared in Figure 18.

For the clean model, the drag coefficients measured in the IRT are high compared with the dry aerodynamic tunnel data. There were some differences in the Reynolds and Mach numbers at which the data was taken in the two tunnels (Re = 9.1 million and M = 0.20 in F1 versus Re = 10.4 million and M = 0.235 in IRT), but the primary difference was the higher turbulence levels in the IRT.

The ice accretion case that matched an ice casting tested at the F1was for a 2 min exposure time. At low angles of attack, 0° and 2°, the drag coefficients measured in the IRT are high. However, for angles of attack of 4° and 6°, the drag coefficients agree well. These results might be explained by: 1) at the lower AoA's for this amount of ice, the drag is predominantly due to skin friction where the higher turbulence level in the IRT has an influence, and 2) at the higher angles, a larger area of the airfoil is covered by the trailing edge separation zone and the effects due to IRT turbulence are less important.

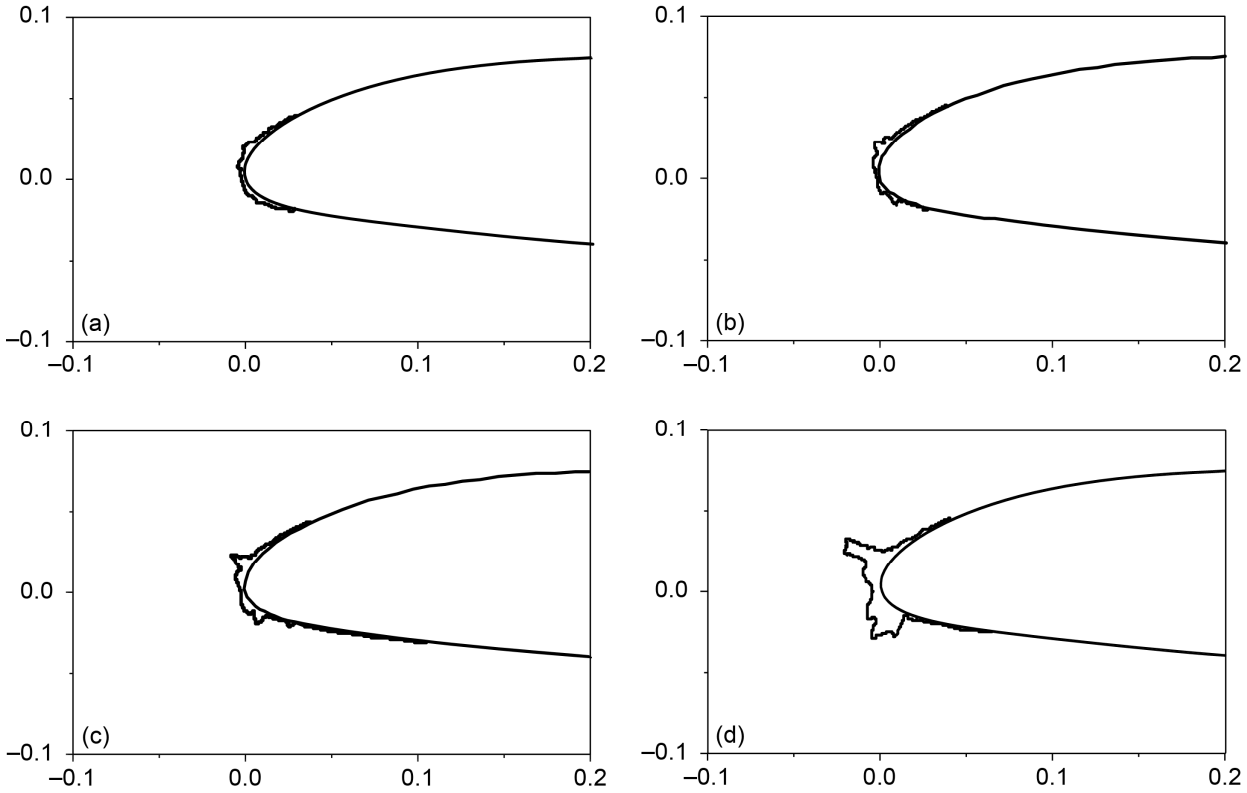

Figure 16.—Ice accretion on 6 ft chord model. (a) 5.0 min. (b) 7.5 min. (c) 10 min. (d) 22.5 min.

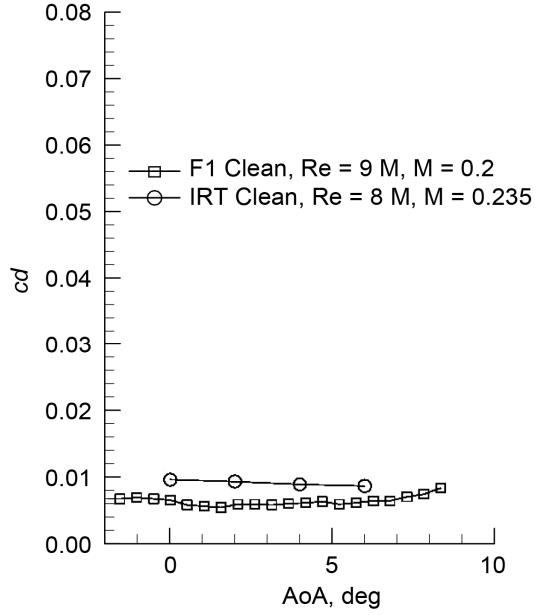

Figure 17.—6 ft chord, clean model data from IRT and F1.

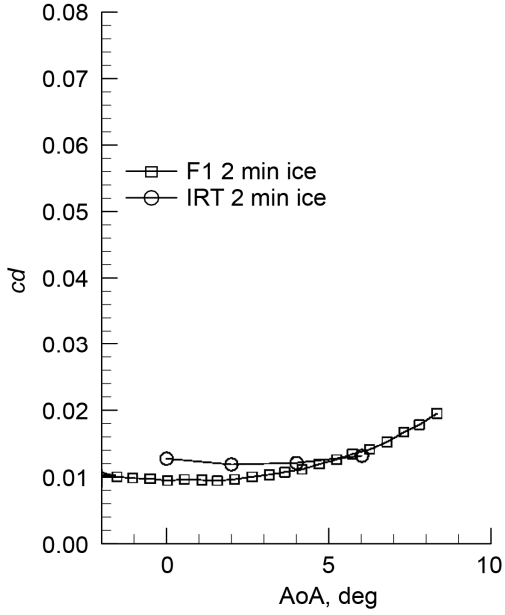

Figure 18.—6 ft chord, iced model drag data from IRT and F1.

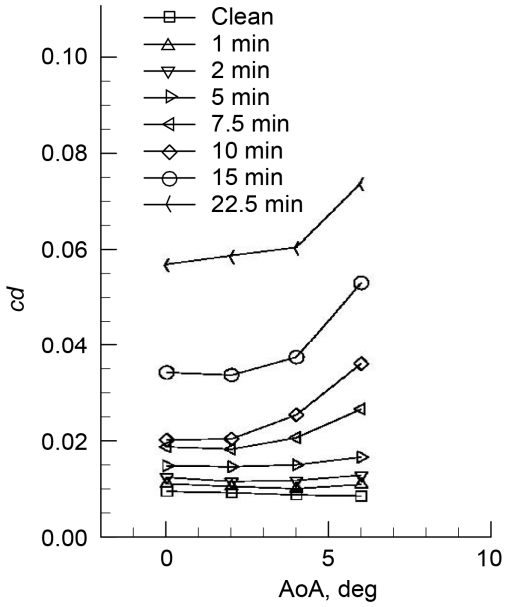

Figure 19.—Iced drag coefficients for 6 ft chord model in IRT.

Since most of the data with the 6 ft chord model in the IRT were acquired with ice accretion times greater than 2 min, the drag results should be reasonable.

The set of drag coefficient curves versus angle of attack for the various icing exposure times is shown in Figure 19.

Normalizing the ice tracings and the models by chord length allows the ice shapes to be compared for geometric similarity. The cross plotted ice shapes for three of the four comparable Ac-beta cases are shown in Figures 20(a) to (c). The ice tracings for Cases B and C are very similar. The tracings for the 6 ft chord model do seem to be a bit rougher, but that may be an artifact of the tracing process. Tracing ice does result in some smoothing of the finer ice roughness. Such roughness may have been smoothed over when tracing the ice on the 1.5 ft chord model, but such features on the 6 ft model were large enough to be traced.

However, there are some differences in the Case D ice shapes, even though, overall, the amount of ice is about the same and there are lower and upper surface horns on both. The upper surface horn on the 6 ft chord model is taller and narrower, and is angled more forward than the ice accretion for the 1.5 ft chord model. The lower surface horn has about the same angle, but is taller and narrower.

Figure 21 shows the drag coefficient versus angle of attack curves plotted along with the curves from the first campaign for the clean airfoils as well as for the iced airfoils with similar Ac-beta values. The clean airfoil drag curves agree well. The Ac-beta Case B and C curves also agree well with the drag values from the 1.5 ft chord model. However, neither the Case A nor the Case D drag curves agree well with the curves from the 1.5 ft chord model. For Case A, the drag values for the 1.5 ft chord model were significantly higher than for the 6 ft chord model. These data confirm the suspicion mentioned earlier that drag for an initial ice shape on the 1.5 ft airfoil was too high and not representative of an initial ice accretion on a full scale airfoil. For Case D, however, the drag coefficients from the 6 ft chord model are much higher than those from the 1.5 ft chord model tests. This result was not expected.

The higher than expected drag coefficients for the longer icing exposures are also evident when plotting the 6 ft chord model data versus exposure time as shown in Figure 22. Unlike the curves for the 1.5 ft model as shown in Figure 14, the curves form straight lines for the shorter icing duration periods. However, there is a noticeable break in the slope of the curves at the icing exposure time of 10 min for the angles of attack of 0° and 2° and 5 min for the angles of attack of 4° and 6°.

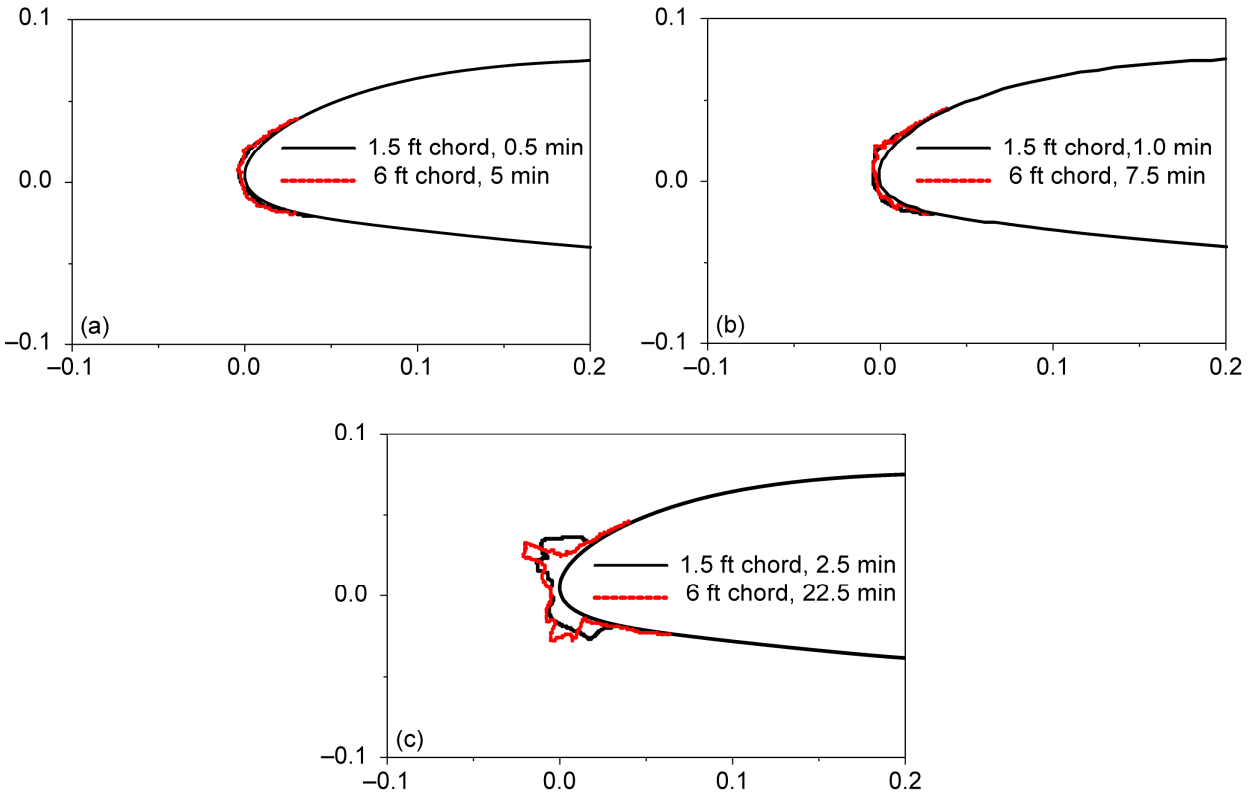

Figure 20.—Ice tracings for similar ice accretion cases for 1.5 and 6 ft chord models. (a) Case B. (b) Case C. (c) Case D.

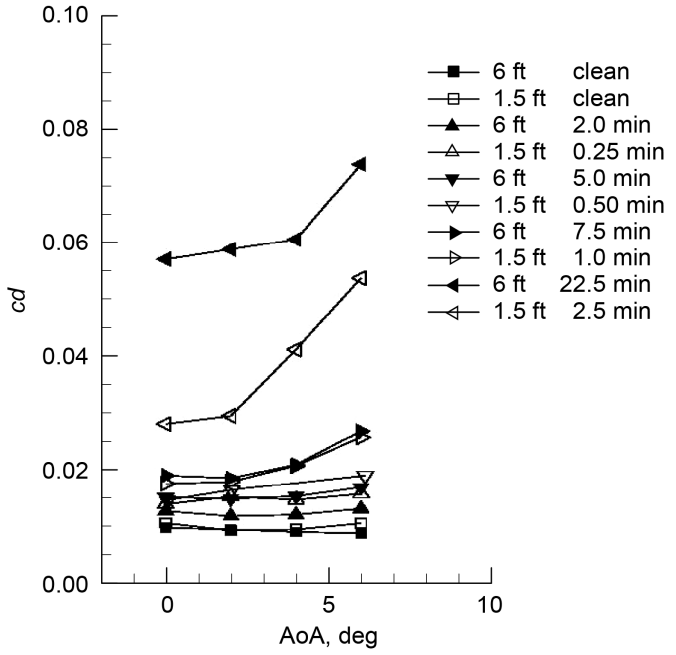

Figure 21.—Drag coefficients for ice accretions with similar Ac-beta values for both 1.5 and 6 ft chord models.

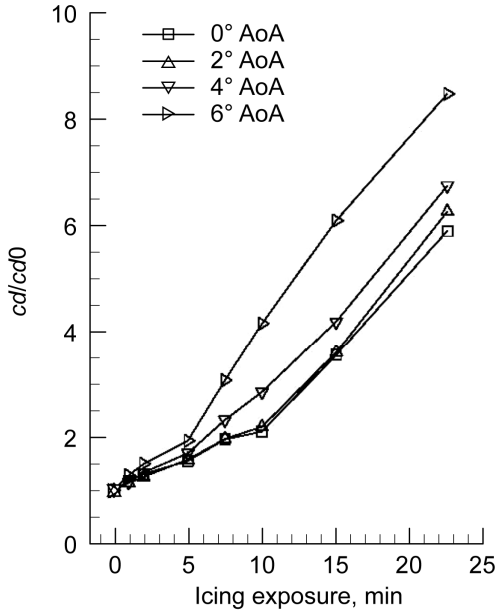

Figure 22.—Normalized drag coefficients for 6 ft chord.

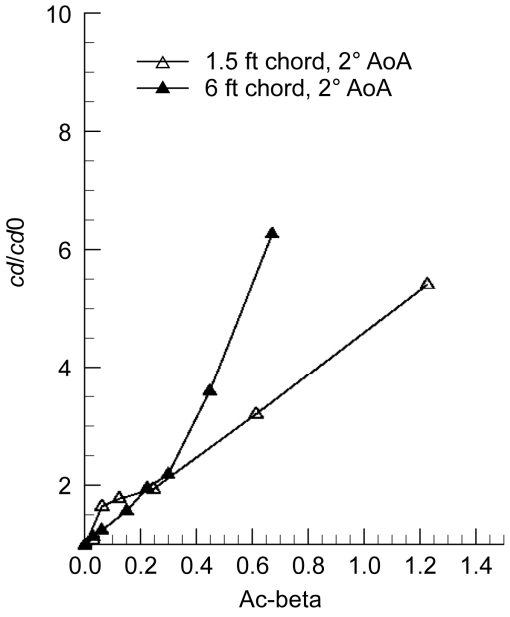

Figure 23.—Normalized drag coefficients for iced 1.5 and 6 ft chord models at 2° AoA as a function of accumulation parameter x collection efficiency.

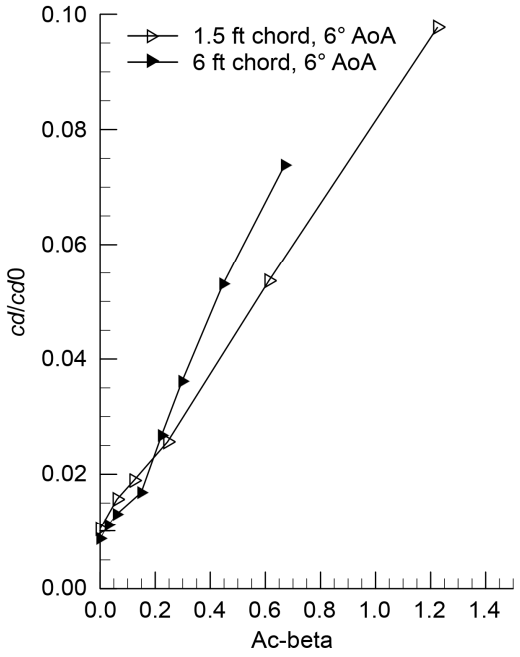

Figure 24.—Normalized drag coefficients for iced 1.5 and 6 ft chord models at 6° AoA as a function of accumulation parameter x collection efficiency.

This observation is also demonstrated in the plot of normalized drag coefficient versus Ac-beta for both models at 2° AoA, as shown in Figure 23. In this plot, the higher drag values for the 1.5 ft chord model at lower Ac-beta values are easily seen as are the much greater drag values for the 6 ft chord model at the higher Ac-beta values. It indicates that something about the larger ice shapes on the 6 ft chord model is having a significantly different effect on aerodynamic drag.

The difference in drag for larger ice shapes between the two models is also seen in Figure 24 where drag values for the two airfoils are plotted versus Ac-beta, only this time at 6° angle of attack. Here, the difference in drag appears at Ac-beta values as low as 0.2. These data reflect the increasing importance of the upper surface horn to the airflow at higher angles of attack. The reader will note that, at low Ac-beta values, the curves for the two models agree. This suggests that the increase in drag for the smaller model at short icing exposure times is due to ice on the lower surface of the airfoil.

For each ice tracing made in the IRT, an ice depth gage was used to measure the maximum thickness of ice on both the upper and lower airfoil surfaces. The thickness of the ice at the stagnation line was also measured. These measurements are shown in Table 2 along with the corresponding values normalized by chord length, k/c. The k/c values are also plotted as a function of Ac-beta in Figures 25 and 26. Figure 25 shows the upper surface and stagnation line values for both models. The stagnation line values for the two models agree well. This is not surprising because icing scaling methods are based upon stagnation line similarity assumptions. The normalized upper surface maximum ice thickness values for the 6 ft chord model are, however, higher than those for the 1.5 ft chord model. This result is likely due to the complexity of the glaze ice accretion process where airspeed, air temperature, amount of water, and boundary layer dynamics all play a role in where the flowing water freezes as it flows downstream. Such details are difficult, if not impossible, to capture in icing scaling methods.

Maximum ice thickness data for the lower surface are shown in Figure 26. The data for the two models match remarkably well for accretions up to an Ac-beta value of 0.30. This corresponds to the 10 min ice accretion for the 6 ft chord model. It also corresponds to the point where the slope changes in the normalized drag versus icing exposure time curves for 0° and 2° AoA in Figure 22 as well as in the 6 ft chord model normal drag versus Ac-beta curve of Figure 23.

TABLE 2.—ICE THICKNESS DATA

Two-dimensional NACA-23012									
Chord	Exp. time	Ac-beta	Ice Thickness, in.			k/c			Similar cases
ft	min		Upper	Stagnation	Lower	(upper)	(stag)	(lower)	
1.5	0.25	0.061	-------	-------	-------	-------	-------	-------	A
1.5	0.5	0.12	0.04	0.03	0.03	0.002	0.002	0.002	B
1.5	1	0.25	0.11	0.05	0.12	0.0061	0.0028	0.0067	C
1.5	2.5	0.61	0.39	0.09	0.27	0.022	0.005	0.015	D
1.5	5	1.2	0.81	0.15	0.53	0.045	0.0083	0.029	
6	1	0.030	-------	-------	-------	-------	-------	-------	
6	2	0.060	-------	-------	-------	-------	-------	-------	A
6	5	0.15	0.42	0.12	0.25	0.0058	0.0017	0.0035	B
6	7.5	0.22	0.64	0.17	0.44	0.0089	0.0024	0.0061	C
6	10	0.30	0.92	0.18	0.6	0.013	0.0025	0.0083	
6	15	0.45	1.28	0.28	0.96	0.0178	0.0039	0.0133	
6	22.5	0.67	1.88	0.38	1.71	0.0261	0.0053	0.0238	D

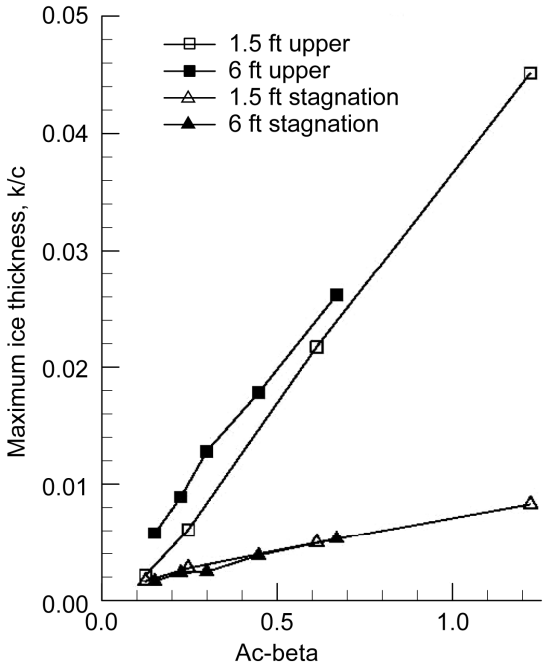

Figure 25.—Maximum ice thickness on the upper surface and at the stagnation line normalized by chord length as a function of accumulation parameter x collection efficiency.

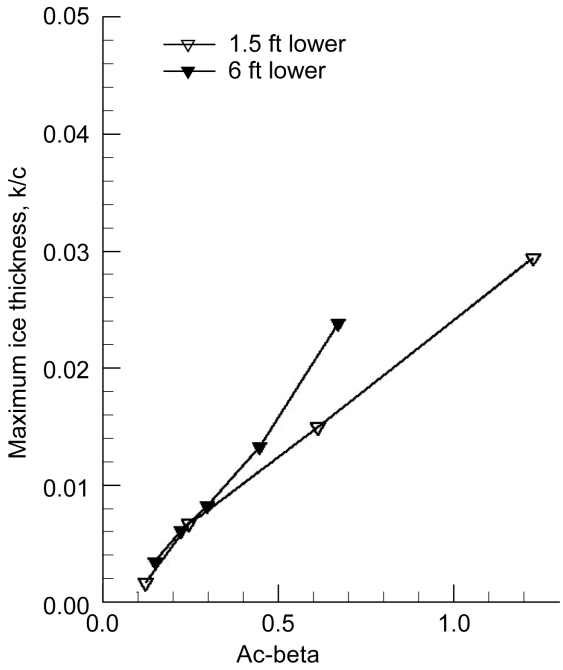

Figure 26.—Maximum ice thickness on the lower surface normalized by chord length as a function of accumulation parameter x collection efficiency.

These observations indicate that the character of the ice for the longer exposure times on the 6 ft chord model is responsible for the higher drag values when compared with those of the 1.5 ft chord model. The upper surface horn on the 6 ft chord model is slightly higher, less-rounded, and has a slightly different position on and angle with respect to the local surface than the upper surface horn on the 1.5 ft chord model. Furthermore, it is interesting and important to note that in both the case of the 1.5 ft chord model with the initial ice accretion and in the case of the 6 ft chord airfoil with the long-exposure ice accretion, it is the character of the ice that results in increased drag.

A further observation from the data of this study is that not only are features of the ice important, but when during the ice accretion they begin to take shape is important. The drag for the 6 ft airfoil increased at an accelerated rate once both upper and lower surface horns were established.

Finally, the novel analysis of aerodynamic performance in terms of parameters typically used of icing scaling provides a means to assess the level of fidelity required for effective icing simulation.

Concluding Remarks

The primary objective of this study was to investigate how aerodynamic performance degrades as ice accretes on an airfoil. Existing two-dimensional airfoil models were used which had an established background of ice-contaminated aerodynamic performance data. Glaze icing conditions were selected which had shown to be particularly detrimental to aerodynamic performance.

The two models used in the study were both NACA-23012 airfoils. The difference between them was size. The smaller model had a chord of 1.5 ft while the larger one had a chord of 6 ft; typical of airfoils of this family in use on aircraft. The smaller model was used because it could be rotated through stall in the NASA Icing Research Tunnel. The larger model could not without inducing undue blockage in the tunnel. Both models had a floor-to-ceiling span of 6 ft.

Results from the small model testing showed that maximum lift coefficient and stall angle degraded in a diminishing manner as time exposed to icing conditions increased. In general, drag coefficient increased linearly with time exposed to icing conditions, with the exception of short exposure times where increases in drag coefficient were more pronounced.

Only aerodynamic drag results were available from the tests with the large, 6 ft chord model. For these tests, the large model could not be mounted to the IRT's external force balance and ice covered surface pressure taps needed to make accurate performance calculations. Due to the large model's lower collection efficiency, slight changes were made to cloud droplet size, liquid water content, and exposure times to result in geometrically similar ice accretions as in the smaller model test.

Results from the large model test showed that drag initially increases linearly with icing exposure time but, for longer ice accretion times, it increases more rapidly. The cause of this behavior appeared to be the establishment of relatively taller and narrower ice horns on the upper and lower surfaces of the airfoil at certain points during exposure to icing conditions. These ice features were different from those which formed on the small scale airfoil and were likely the reason for differences in drag coefficients measured on the two airfoils even though the ice shapes were relatively similar. Furthermore, the study emphasized that not only are particular ice features important, but also the point in time during an icing encounter when they develop is important.

In order to compare the data between the subscale and full scale airfoils, aerodynamic performance data were assessed using icing scaling parameters. The correlations provide a novel manner in which icing data can be analyzed. Moreover, it provides a means by which the fidelity of icing simulations can be assessed; a goal that has remained elusive in icing technology.

References

1. Bragg, M., Broeren, A., Addy, H., Potapczuk, M., Guffond, D., Montreul, E., "Airfoil Ice-Accretion Aerodynamics Simulation," AIAA–2007–0085, 2007.
2. Papadakis, M., Yeong, H.W., Vargas, M., Potapczuk, M.P., "Aerodynamic Performance of a Swept Wing with Ice Accretions," AIAA–2003–731, January 2003.
3. Papadakis, M., Gile-Laflin, B.E., "Aerodynamic Performance of a T-tail with Simulated Ice Accretions," January 2000.
4. Papadakis, M., Alansatan, S., Yeong, H.W., "Aerodynamic Performance of a Swept Wing with Ice Accretions," AIAA–2003–731, January 2003.
5. Addy, H.E., Broeren, A., Zoeckler, J., Lee, S., "A Wind Tunnel Study of Icing Effects on a Business Jet Airfoil," AIAA–2003–727, January 2003.
6. Addy, H.E., Chung, J.J., "A Wind Tunnel Study of Icing Effects on a Natural Laminar Flow Airfoil," AIAA–2000–95, January 2000.
7. Addy, Jr., H.E., "Ice Accretions and Icing Effects for Modern Airfoils," NASA/TP—2000-210031, DOT/FAA/AR-99/89, April 2000.
8. Addy, H.E., Potapczuk, M.G., Sheldon, D.W., "Modern Airfoil Ice Accretions," AIAA–1997–174, January 1997.
9. Busch, G., Broeren, A., Bragg, M., "Aerodynamic Fidelity of Sub-scale Two-Dimensional Ice Accretion Simulations," AIAA–2008–7062, 2008.
10. Broeren, A.P., Bragg, M.B., "Aerodynamics of Ice Remnants from Protected Surfaces," AIAA–2006–0259, January 2006.
11. Busch, G., Broeren, A., Bragg, M., "Aerodynamic Simulation of a Horn-Ice Accretion on a Subscale Model," AIAA–2007–0087, January 2007.
12. Broeren, A.P., Addy, H.E., Bragg, M.B., "Effect of Intercycle Ice Accretions on Airfoil Performance," AIAA–2002–0240, January 2002.
13. Whalen, E.A., Broeren, A.P., Bragg, M.B., "Aerodynamics of Scaled Runback Ice Accretions," *Journal of Aircraft*, vol. 45, no. 2, March-April 2002, pp. 591–603.Kim, H.S., Bragg, M.B., "Effects of Leading-Edge Ice Accretion Geometry on Airfoil Aerodynamics," AIAA 99-3150, June 1999.
14. Lee, S., Kim, H.S., Bragg, M.B., "Investigation of Factors that Influence Iced-Airfoil Aerodynamics," AIAA–2000–0099, January 2000.
15. Lee, S., Dunn, T., Gurbacki, H.M., Bragg, M.B., Loth, E., "An Experimental and Computational Investigation of Spanwise-Step-Ice Shapes on Airfoil Aerodynamics," AIAA No. 98-0490, January 1998.
16. Cook, D.E., "Relationships of Ice Shapes and Drag to Icing Condition Dimensionless Parameters," AIAA–2000–0486, January 2000.
17. Potapczuk, M.G., Berkowitz B.M., "An Experimental Investigation of Multi-Element Airfoil Ice Accretion and Resulting Performance Degradation," AIAA–89–0752, January 1989.
18. Gonsalez, J.C., Arrington E.A., "Aerodynamic Calibration of the NASA Lewis Icing Research Tunnel (1987 Test)," AIAA–98–0633, January 1998.
19. Wright, W.B., Rutkowski, A., "Validation Results for LEWICE 2.0," NASA/CR—1999-208690, January 1999.
20. Rae, Jr., R.H., and Pope, A., *Low-Speed Wind Tunnel Testing*, 2nd ed., John Wiley & Sons, New York, 1984, pp. 249.
21. Anderson, D.N., "Manual of Scaling Methods," NASA/CR—2004-212875, March 2004.
22. Shin, J., and Bond, T.H., "Repeatability of Ice Shapes in the NASA Lewis Icing Research Tunnel," *Journal of Aircraft,* vol. 31, no. 5, pp. 1057–1063.

REPORT DOCUMENTATION PAGE		Form Approved OMB No. 0704-0188

1. REPORT DATE *(DD-MM-YYYY)*	2. REPORT TYPE	3. DATES COVERED *(From - To)*
01-03-2011	Technical Memorandum	

4. TITLE AND SUBTITLE
Icing Encounter Duration Sensitivity Study

5a. CONTRACT NUMBER

5b. GRANT NUMBER

5c. PROGRAM ELEMENT NUMBER

6. AUTHOR(S)
Addy, Harold, E., Jr.; Lee, Sam

5d. PROJECT NUMBER

5e. TASK NUMBER

5f. WORK UNIT NUMBER
WBS 457280.02.07.03.02.02

7. PERFORMING ORGANIZATION NAME(S) AND ADDRESS(ES)
National Aeronautics and Space Administration
John H. Glenn Research Center at Lewis Field
Cleveland, Ohio 44135-3191

8. PERFORMING ORGANIZATION REPORT NUMBER
E-17303

9. SPONSORING/MONITORING AGENCY NAME(S) AND ADDRESS(ES)
National Aeronautics and Space Administration
Washington, DC 20546-0001

10. SPONSORING/MONITOR'S ACRONYM(S)
NASA

11. SPONSORING/MONITORING REPORT NUMBER
NASA/TM-2011-216367

12. DISTRIBUTION/AVAILABILITY STATEMENT
Unclassified-Unlimited
Subject Categories: 02 and 03
Available electronically at http://sti.nasa.gov
This publication is available from the NASA Center for AeroSpace Information, 443-757-5802

13. SUPPLEMENTARY NOTES

14. ABSTRACT
This paper describes a study performed to investigate how aerodynamic performance degradation progresses with time throughout an exposure to icing conditions. It is one of the first documented studies of the effects of ice contamination on aerodynamic performance at various points in time throughout an icing encounter. Both a 1.5 and 6 ft chord, two-dimensional, NACA-23012 airfoils were subjected to icing conditions in the NASA Icing Research Tunnel for varying lengths of time. At the end of each run, lift, drag, and pitching moment measurements were made. Measurements with the 1.5 ft chord model showed that maximum lift and pitching moment degraded more rapidly early in the exposure and degraded more slowly as time progressed. Drag for the 1.5 ft chord model degraded more linearly with time, although drag for very short exposure durations was slightly higher than expected. Only drag measurements were made with the 6 ft chord airfoil. Here, drag for the long exposures was higher than expected. Novel comparison of drag measurements versus an icing scaling parameter, accumulation parameter times collection efficiency was used to compare the data from the two different size model. The comparisons provided a means of assessing the level of fidelity needed for accurate icing simulation.

15. SUBJECT TERMS
Aircraft icing; Aerodynamic performance; Icing exposure duration

16. SECURITY CLASSIFICATION OF:			17. LIMITATION OF ABSTRACT	18. NUMBER OF PAGES	19a. NAME OF RESPONSIBLE PERSON
a. REPORT	b. ABSTRACT	c. THIS PAGE			STI Help Desk (email:help@sti.nasa.gov)
U	U	U	UU	24	19b. TELEPHONE NUMBER *(include area code)* 443-757-5802